Gorazd ŠTUMBERGER[1],Klemen DEŽELAK[1], Beno KLOPČIČ[1,2], Drago DOLINAR[1]

University of Maribor, Slovenia (1)
Indramat elektromotorji d.o.o., Slovenia (2)

Acoustic noise emissions caused by the transformer in a DC/DC converter for welding applications

***Abstract**. This paper focuses on acoustic noise emissions caused by the transformer that operates as a part of DC/DC converter installed in a resistance spot welding system (RSWS). The discussed RSWS contains a three-phase input rectifier, an inverter, an iron core welding transformer with one primary and two secondary winding and two output rectifier diodes connected to the transformer's secondary windings. In the case study, two different methods are applied to generate the inverter output voltage, which supplies the transformer's primary winding. Considering possible origins of acoustic noise emission in the discussed transformer and based on performed simulations and measurements, the paper explains while the two applied voltage generation methods influence the acoustic noise emissions caused by the transformer differently.*

***Streszczenie.** W artykule opisano zagadnienie emisji hałasu przez transformator pracujący w układzie przetwornicy DC/DC w spawarce punktowej (ang. Resistance Spot Welding - RSW). Omawiana spawarka składa się z prostownika trójfazowego, falownika i transformatora z rdzeniem żelaznym. W badaniach wykorzystano dwie metody generowania napięcia wyjściowego falownika, zasilającego transformator i określono wpływ każdej z nich na emisję hałasów. (**Emisja hałasu przez transformator pracujący w układzie przetwornicy DC/DC w spawarce**).*

Keywords: DC/DC converter, transformer, acoustic noise emissions.
Słowa kluczowe: przetwornica DC/DC, transformator, emisja hałasu.

Introduction

Generally, electromagnetic devices supplied by varying currents emit acoustic noise. If the impacts on human health are not discussed, the acoustic noise emissions caused by the electromagnetic devices could be found in the range from imperceptible to annoying and even distracting. In order to keep the acoustic noise emissions caused by an electromagnetic device in an acceptable range, the origin of acoustic noise must be known.

This paper deals with the accoustic noise emission caused by the welding transformer, operating as a part of DC/DC converter in a resistance spot welding system (RSWS). Generally, the acoustic noise produced by a transformer can originate from the winding vibrations, from the iron core vibrations or from both of them [1]. The winding vibration can be caused by periodical mutual forces acting on current-carrying conductors. Vibration of the entire iron core is often provoked by magnetostriction while vibration of the iron core pieces can appear due to periodically-changing magneto motive forces acting across the air gaps. According to [2], the magnetostriction can be described as the change in length or shape of ferromagnetic material under magnetization.

The authors in [3] deal with different numerical models for the calculation of vibrations in iron cores. The impact of megnetostriction on the acoustic noise emissions caused by the iron cores of transformers is evaluated in [4]. The authors in [5] use measurement to evalute vibrations and acoustic noise emissions, caused by the iron core of a three-phase three-limb transformer supplied by sinusoidal and pulse width modulation (PWM) generated voltages. Magnetic field analysis, calculation of nodal forces and vibration analysis are applied in [6] to evaluate the acoustic noise emissions caused by an inverter driven single-phase inductor. The development of a ultra-low-noise transformer technology, based on the calculation and measurements of iron core resonant frequencies, frequency spectrum of iron core noise, and load noise, is presented in [7].

The welding transformer treated in this paper operates as a part of DC/DC converter installed in an industrial RSWS. The discussed DC/DC converter is schematically shown in Fig. 1. It consists of an input rectifier, an H-bridge inverter, welding transformer and output rectifier. The input rectifier converts the three-phase input voltages u_1, u_2 and u_3 into a smooth and almost constant DC-bus voltage U_{DC}. It supplies the H-bridge inverter that fed the transformer's primary windings with voltage pulses u_H. One primary and two secondary windings are wound around transformer's iron core. The output rectifier diodes (D_1 and D_2), mounted on both transformers' secondary windings, are used to provide the direct welding current i_L flowing through the load represented by the inductance L_L and the resistance R_L.

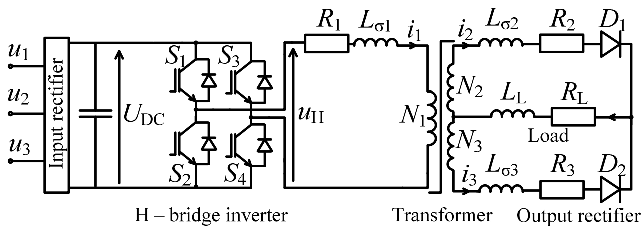

Fig.1. Schematic presentation of discussed RSWS

The analysis of discussed RSWS performed in [8] has shown, that even under normal operating conditions, the transformer's iron core can become saturated due to the unbalances in both loops with secondary windings and differences in characteristics of output rectifier diodes. It was shown that the iron core saturation can lead to the pretty high current spikes in the primary current of the transformer, which finally cause the overcurrent protection switch-off of the entire system. Two different methods, which can be used for active prevention of transformer's iron core form becoming saturated, are discussed in [9]. Both methods require closed-loop control of the welding current and iron core flux density. The first method uses two proportional–integral (PI) controllers to control the welding current and the DC component of iron core flux density in the closed-loop, while a modified pulse-width-modulation (PWM) is used to generate the H-bridge inverter output voltage. The second method uses two synchronously operating hysteresis controllers to simultaneously closed-loop control the welding current and the saturation level in the iron core, and to generate the H-bridge inverter output voltages [10,11]. During the testing of methods and corresponding control scheme introduced in [9,10,11], it became evident that the control scheme [10] not only improves utilization of the iron core and prevent it from becoming saturated, but also substantially reduces the acoustic noise emissions caused by the transformer. The reasons for reduction of acoustic noise emission are analysed in this paper.

System description

Individual components of the discussed RSWS, shown in Fig. 1, were described in the previous section. Let us focus on the welding transformer and RSWS dynamic model. The transformer has one primary winding and two secondary windings denoted with indices 1, 2 and 3, respectively. Thus, R_1, R_2 and R_3 are the resistances; $L_{\sigma 1}$, $L_{\sigma 2}$ and $L_{\sigma 3}$ are the leakage inductances; N_1, N_2 and N_3 are the numbers of turns, while i_1, i_2 and i_3 are the currents, of the three windings. The voltage balances in individual windings are described by (1) to (3), while (4) describes magnetic balances in the iron core:

$$u_{\mathrm{H}} = R_1 i_1 + L_{\sigma 1}\frac{di_1}{dt} + N_1 S_{\mathrm{Fe}}\frac{dB}{dt} \tag{1}$$

$$N_2 S_{\mathrm{Fe}}\frac{dB}{dt} = -R_2 i_2 - L_{\sigma 2}\frac{di_2}{dt} - D_1(i_2) - R_{\mathrm{L}}(i_2+i_3) - L_{\mathrm{L}}\frac{d(i_2+i_3)}{dt} \tag{2}$$

$$N_3 S_{\mathrm{Fe}}\frac{dB}{dt} = R_3 i_3 + L_{\sigma 3}\frac{di_3}{dt} + D_2(i_3) + R_{\mathrm{L}}(i_2+i_3) + L_{\mathrm{L}}\frac{d(i_2+i_3)}{dt} \tag{3}$$

$$N_1 i_1 + N_2 i_2 - N_3 i_3 = H(B)l + \frac{B}{\mu_0}2\delta \tag{4}$$

where S_{Fe} is the cross-section of the iron core, l is the average length of the magnetic path in the iron core, δ is the air gap along the magnetic path inside the iron core consisting of two C-shaped halves, μ_0 is the permeability of vacuum, H is the magnetic field strength, B is the magnetic flux density, $H(B)$ is the characteristic describing magnetically nonlinear behaviour of the iron core, while $D_1(i_2)$ and $D_2(i_3)$ are the nonlinear characteristic of the output rectifier diodes D_1 and D_2, shown in Fig.1. The supply voltage of the transformer u_{H} is generated by switching-on and -off transistor pairs S_1-S_4 and S_2-S_3 in the H-bridge inverter, where different switching patterns can be applied. Considering U_{DC} as constant, u_{H} can be only equal to $+U_{\mathrm{DC}}$, $-U_{\mathrm{DC}}$ or 0.

The dynamic model given by (1) to (4) was applied to calculate the instantaneous values and amplitude spectra of the welding current i_{L}, the primary current i_1, and the iron core flux density B. They are given for two different methods used for the closed-loop control of the welding current and iron core flux density, which lead to quite different switching patterns for generation of transformer's supply voltage u_{H}. Finally, the acoustic noise emissions of the transformer were measured for both control methods. The analysis of calculated and measured amplitude spectra of i_{L}, i_1, B, and the sound pressure level SPL helped us to understand why the applied control method influence the acoustic noise emissions of the welding transformer differently.

The sound pressure level SPL (5) is the measure for evaluation of acoustic noise emissions:

$$SPL = 10\log_{10}\frac{p_{\mathrm{RMS}}^2}{p_{\mathrm{ref}}^2} = 20\log_{10}\frac{p_{\mathrm{RMS}}}{p_{\mathrm{ref}}} \tag{5}$$

where p_{ref} is the reference sound pressure, whilst p_{RMS} is the measured RMS sound pressure.

Control method I: PI controllers and PWM

The welding current i_{L} is controlled with the root mean square (RMS) value of the supply voltage u_{H}, while the dc component of the iron core flux density is controlled by the dc component of u_{H} [11]. The differences between the reference and measured values are used to closed-loop control the welding current and dc component of the iron core flux density by two PI controllers. The output of the welding current PI controller is U_{ref} , while the output of the iron core flux density dc component controller is ΔU. The output voltage of H-bridge inverter u_{H} is PWM generated as shown in Fig. 2, while T_{p} denotes one cycle of modulation. Fig. 2 shows how the voltages U_{ref} and ΔU are combined in the reference voltage u_{ref}. After it is comparation with the carrier signal u_{t}, the control signals u_{m}, that switches-on and -off H-bridge inverter transistor pairs S_1-S_4 and S_2-S_3, is generated. The transistor pair S_1-S_4 is switched-on and -off for the time $t \in [0, T_{\mathrm{p}}/2]$, while for the time $t \in [\,[T_{\mathrm{p}}/2, T_{\mathrm{p}}]$ the transistor pair S_2-S_3 is switched-on and -off. The voltage U_{ref} influences the RMS value of u_{H} while the voltage ΔU influences its dc component.

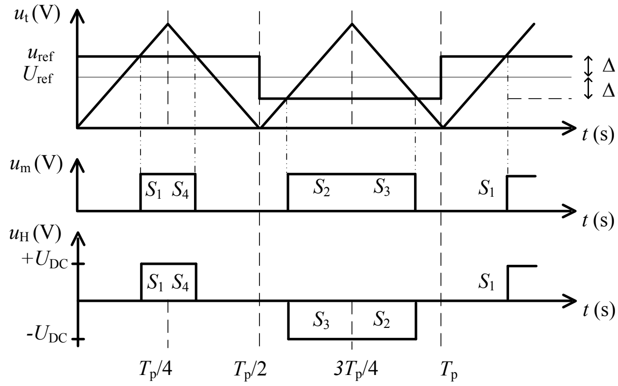

Fig. 2. Control method I: generation of voltage u_{H}

Control method II: Advanced hysteresis control

For constant DC-bus voltage U_{DC}, the H-bridge inverter output voltage $u_{\mathrm{H}}=U_{\mathrm{DC}}$ when the transistor pair S_1-S_4 is switched-on and $u_{\mathrm{H}}=-U_{\mathrm{DC}}$ when the transistor pair S_2-S_3 is switched-on. The iron core flux density B increases for $u_{\mathrm{H}}=U_{\mathrm{DC}}$ and decreases for $u_{\mathrm{H}}=-U_{\mathrm{DC}}$. The welding current i_{L} increases when $u_{\mathrm{H}}\neq 0$ and decreases when $u_{\mathrm{H}}=0$. The aplied control method II is schematically shown in Fig. 3 and described in [9-11].

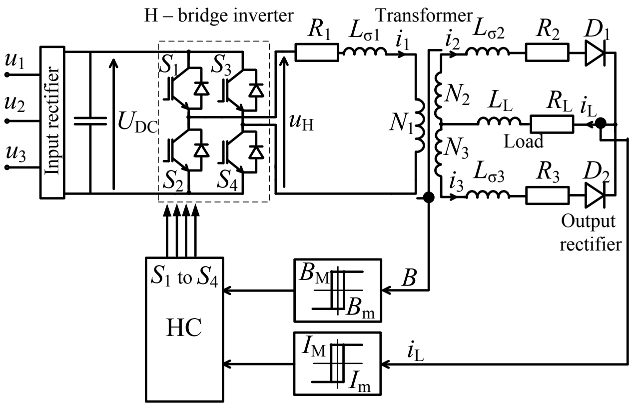

Fig. 3. Control method II: generation of voltage u_{H}

The the welding current i_{L} and iron core flux density B are measured to be closed-loop controlled by two hysteresis controllers. The lower and upper bounds for the welding current and flux density hysteresis controllers are set to [I_{m}, I_{M}] and [$-B_{\mathrm{m}}$, B_{m}], respectively. B_{m} is the flux density value where the iron core starts to become saturated. The flux density controller changes the polarity of u_H when B exceeds the lower or upper bounds while the welding current controller switches the voltage u_H off when i_L exceeds the upper bound I_M and it switches it on again when i_L drops under the lower bound I_m.

Results

Figs. 4 show the time behaviours of i_L, i_1 and B, as well as their amplitude spectra, given as functions of the harmonic component h, calculated by the model (1)-(4), in the case of control method I.

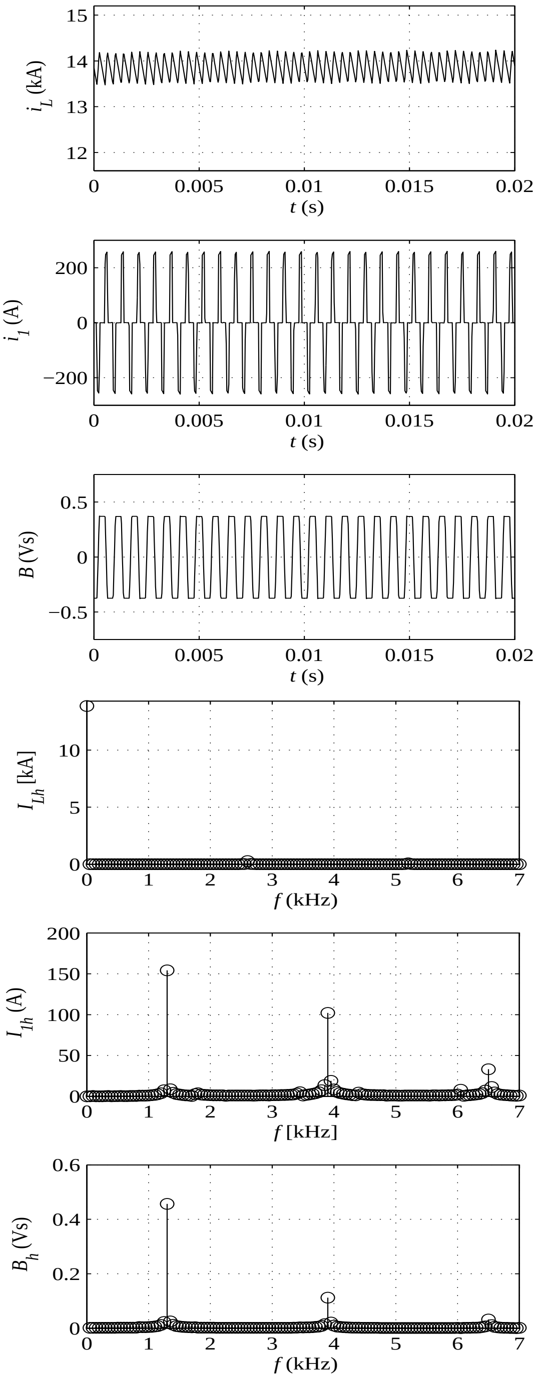

Fig. 4. Control method I: calculated welding current i_L and its amplitude spectrum I_{Lh}; calculated primary currant i_1 and its amplitude spectrum I_{1h}; calculated iron core flux density B and its amplitude spectrum B_h.

Similarly, Figs. 5 show the time behaviours of i_L, i_1 and B, as well as their amplitude spectra, calculated by the model (1)-(4), in the case of control method II. The amplitude spectra of *SPL* measured on the actual RSWS, where the control methods I and II were applied, are shown in Fig. 6.

The results presented in Figs. 4 to 6 clearly show, that in the case of control method I, the primary current i_1 and the iron flux density B have strong spectral lines at the same frequency of 1.3 kHz, which results in the strong spectral line in the sound pressure level *SPL* at 2.6 kHz. It could be concluded that in this case the acoustic noise emissions are caused by the vibrations of the primary winding and individual pieces of the iron core, which all together produce really annoying noise.

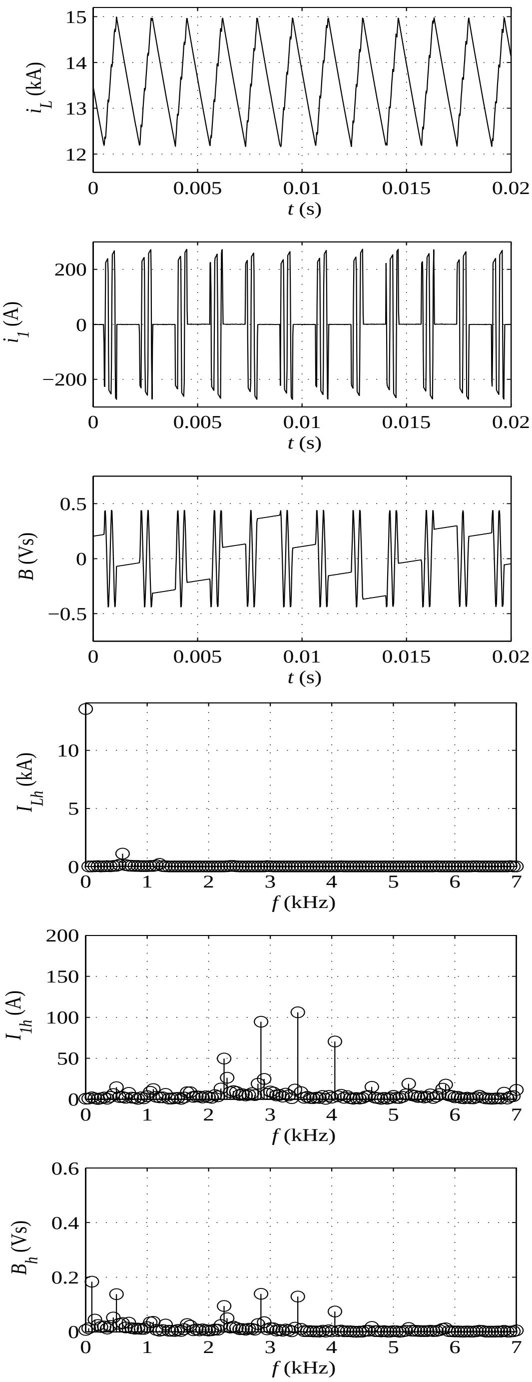

Fig. 5. Control method II: calculated welding current i_L and its amplitude spectrum I_{Lh}; calculated primary currant i_1 and its amplitude spectrum I_{1h}; calculated iron core flux density B and its amplitude spectrum B_h.

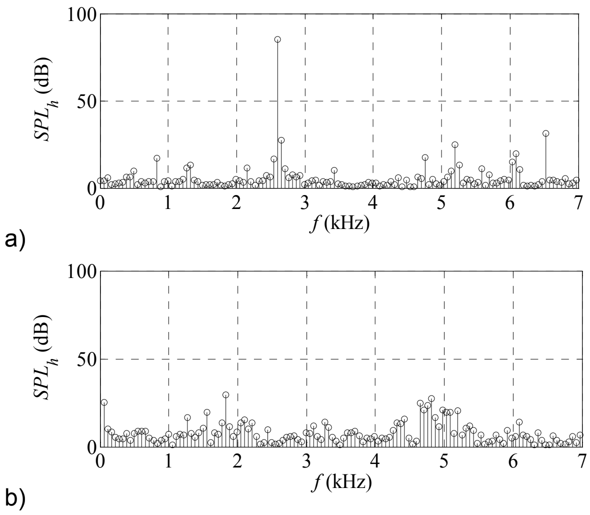

Fig. 6. Amplitude spectrum SPL_h of measured sound pressure level *SPL* for the control method I a) and fo the control method II b)

In the case of control method II, the spectral lines in the primary current and iron core flux density are less strong and they are not limited on only one or two dominant frequencies only. The amplitude spectra are more flat, which leads also to the SPL amplitude spectrum without strongly expressed individual spectral lines. The result is much less annoying noise produced by the welding transformer.

Conclusion

This paper deals with acoustic noise emissions caused by a welding transformer operating as a part of resistance spot welding system. The results of simulations and measurements have shown that the control method II causes much more dispersed amplitude spectra in the primary current and in the iron core flux density, which finally leads also to the dispersed *SPL* amplitude spectra and lower and less annoying acoustic noise emissions. On the contrary, the control method I causes only one really strong spectral lines in the primary current and in the iron core flux density, which appear at the same frequency. This results in a strong spectral line in the SPL amplitude spectrum at doubled frequency, which results in strong and extremely annoying acoustic noise emissions.

REFERENCES

[1] A. W Kelley, “Measurement of spacecraft power transformer acoustic noise,” *IEEE Transactions on Magnetics*, 1990, vol. 26, no. 1, pp. 281-289

[2] T.P.P. Phway and A.J. Moses, “Magnetisation-induced mechanical resonance in electrical steels,” Journal of Magnetism and Magnetic Materials, 2007, vol. 316, pp. 468-471

[3] T. Hilgert, L. Vandevelde, and J. Melkebeek, “Comparison of magneto-striction models for use in calculations of vibrations in magnetic cores,” *IEEE Transactions on Magnetics*, 2008, vol. 44, no. 6, pp. 874-877

[4] B. Weiser, H. Pfützner, and J. Anger, “Relevance of magnetostriction and forces for the generation of audible noise of transformer cores,” *IEEE Transactions on Magnetics*, 2000, vol. 36, no. 5, pp. 3759-3777

[5] X. G. Yao et al., “Magneto-mechanical resonance in a model 3-phase 3-limb transformer core under sinusoidal and PWM voltage excitation,” *IEEE Transactions on Magnetics*, 2008, vol. 44, no. 11, pp. 4111-4114.

[6] Y. Gao, et al., “Vibration analysis of a reactor driven by an inverter power supply considering electromagnetism and magnetostriction,” *IEEE Transactions on Magnetics*, 2009, vol. 45, no. 10, pp. 4789-4892

[7] R. S. Girgis, M. S. Bernesjö, S. Thomas, J. Anger, D. Chu, and H. R. Moore, “Development of ultra-low-noise transformer technology,” *IEEE Transactions on Power Delivery*, 2011, Vol 26, no. 1, pp. 228-234

[8] B. Klopčič, D. Dolinar, and G. Štumberger, “Analysis of an inverter-supplied multi-winding transformer with a full wave rectifier at the output,” Journal of Magnetism and Magnetic Materials, 2008, vol. 320, pp. 2929-2934

[9] G. Štumberger, B. Klopčič, K. Deželak, and D. Dolinar, “Prevention of iron core saturation in multi-winding transformers for dc-dc converters,” *IEEE Transactions on Magnetics*, 2010. vol. 46, no. 2, pp. 582-585

[10] EU Patent EP 2 097 912 B1, May 25, 2011, *Method and apparatus for operating a transformer*, Robert Bosch GmbH.

[11] B. Klopčič, D. Dolinar, and G. Štumberger, “Analysis of an inverter-supplied multi-winding transformer with a full wave rectifier at the output,” Journal of Magnetism and Magnetic Materials, 2008, vol. 320, pp. 2929-2934

Authors

Prof. dr. Gorazd Štumberger, univ. dipl. inž. el., University of Maribor, Faculty of electrical engineering and computer science, , Smetanova ulica 17, 2000 Maribor, Slovenia, E-mail: gorazd.stumberger@uni-mb.si;

Assistant prof. dr. Klemen Deželak, univ. dipl. inž. el., University of Maribor, Faculty of electrical engineering and computer science, Smetanova ulica 17, 2000 Maribor, Slovenia, E-mail: klemen.dezelak@uni-mb.si;

Dr. Beno Klopčič, univ. dipl. inž. el., Indramat elektromotorji d.o.o., Kidričeva cesta 81, 4220 Škofja Loka, Slovenia, E-mail: beno.klopcic@boschrexroth.si;

Prof. dr. Drago Dolinar, univ. dipl. inž. el., University of Maribor, Faculty of electrical engineering and computer science, Smetanova ulica 17, 2000 Maribor, Slovenia, E-mail: dolinar@uni-mb.si;